

# IMPLEMENTATION OF $\beta_N$ CONTROL IN THE NATIONAL SPHERICAL TORUS EXPERIMENT

S. P. GERHARDT,\* D. MASTROVITO, M. G. BELL, M. CROPPER, D. A. GATES, E. KOLEMEN, J. LAWSON, B. MARSALA, J. E. MENARD, D. MUELLER, and T. STEVENSON

Princeton Plasma Physics Laboratory, P.O. Box 451, Princeton, New Jersey 08543

Received October 5, 2010

Accepted for Publication December 6, 2010

*We have designed and constructed a system for control of the normalized  $\beta$  ( $\beta_N$ ) in the National Spherical Torus Experiment [M. Ono et al., Nucl. Fusion, Vol. 40, p. 557 (2000)]. A proportional-integral-derivative operator is applied to the difference between the present value of  $\beta_N$  (from real-time equilibrium reconstruction) and a time-dependent request in order to calculate the required injected power. This injected power request is then turned*

*into modulations of the neutral beams. The details of this algorithm are described, including the techniques used to develop the appropriate control gains. Example uses of the system are shown.*

**KEYWORDS:** NSTX, spherical torus, neutral beam injection

*Note: Some figures in this paper are in color only in the electronic version.*

## I. INTRODUCTION

To be viable as a candidate for fusion energy generation, tokamaks must operate without disruptions.<sup>1</sup> These events, which involve the rapid loss of the plasma-stored energy followed by a fast quench of the plasma current, can cause severe damage to the tokamak in-vessel components, potentially necessitating costly repairs in future devices. There are many causes of disruptions, including plasma instabilities that occur when the plasma pressure becomes too great.

The plasma pressure is typically quoted as normalized to the toroidal magnetic field strength at the average midplane radius of the plasma; this is the toroidal  $\beta$  defined as  $\beta_T = 2\mu_0\langle P\rangle/B_T^2$ , where  $\langle P\rangle$  is the volume-averaged total pressure. It has been found, however, that the toroidal  $\beta$  itself is not a good indicator of proximity to instability; rather, the maximum stable toroidal  $\beta$  scales with  $I_p/aB_T$ , where  $I_p$  is the plasma current in megaamperes and  $a$  is the minor radius in meters (see Ref. 2 and references therein). Hence, we can define a quantity known as the normalized  $\beta$ , given by  $\beta_N = 100aB_T\beta_T/I_p$ . It is this quantity that we wish to regulate in order to both

operate safely near stability boundaries and to enable controlled experiments where other parameters are varied as  $\beta_N$  is held fixed. This paper describes the implementation of a  $\beta_N$  controller for the National Spherical Torus Experiment<sup>3</sup> (NSTX).

The utility of  $\beta_N$  (or stored energy) control has been demonstrated by the implementation of similar systems on other tokamaks. Initial work in this regard was done at Doublet III-D (Ref. 4), Tokamak Fusion Test Reactor (TFTR) (Ref. 5), and Joint European Torus (JET) (Ref. 6). The DIII-D and TFTR cases used the plasma diamagnetism, either directly,<sup>4</sup> or after further processing,<sup>5</sup> as the measurement for feedback. More recent work in this area has been done at JT-60, where a “functional parameterization” method was used to calculate the stored energy in real time<sup>7</sup> from diamagnetic flux and poloidal field measurements; a related study in that device<sup>8</sup> used feedback on the neutron emission rate to adjust the neutral beam injection power to simulate the effect of fusion power heating the plasma. Recent DIII-D studies<sup>9</sup> have extended these studies to simultaneous control of  $\beta_N$  and plasma rotation using the capability provided by having both counter- and co-injecting neutral beams. Control of the plasma current profile with neutral beam injection (and other actuators) has also been demonstrated.<sup>10,11</sup>

\*E-mail: sgerhard@pppl.gov

In this paper, Sec. II describes the hardware and software implementation of the controller, and Sec. III describes the system identification method we have used for determining the appropriate proportional and integral gains. Section IV presents some example uses of the system, with a short discussion following in Sec. V.

## II. CONTROLLER IMPLEMENTATION

### II.A. The NSTX Device and Control System

The  $\beta_N$  control system in NSTX has been implemented as part of the NSTX installation<sup>12,13</sup> of the General Atomics plasma control system<sup>14,15</sup> (PCS), which has overall responsibility for plasma control. This includes control of the plasma current, poloidal and toroidal field coil currents, plasma boundary shape<sup>16</sup> and vertical position, gas fueling, and three-dimensional fields and resistive wall modes.<sup>17–20</sup>

The geometry of the NSTX neutral beam injection system<sup>21</sup> is shown in Fig. 1. The neutral beam injection system on the NSTX was inherited from the TFTR, which used four beamlines injecting up to 33 MW of power.<sup>22</sup> The NSTX has a single neutral beamline, equipped with three sources, injecting parallel to the plasma current. The sources are arranged in a horizontal fan with  $\sim 4$  deg spread between the individual beams. The tangency radii

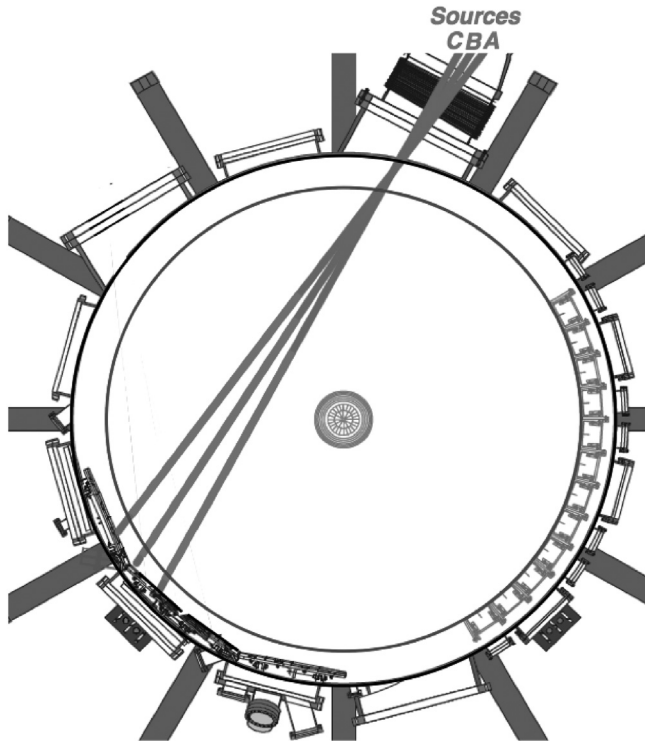


Fig. 1. Schematic of the NSTX neutral beam injection geometry.

of the beams are  $\sim 70$ , 60, and 50 cm for sources A, B, and C, respectively (the typical radius of the magnetic axis is 95 to 105 cm). The sources are typically operated with source voltages between 60 and 95 kV, with 40-kV operation available on request; 110-kV capability has been retained from the TFTR systems but is not used. Note also that source A must be on, with a voltage of 90 kV, in order to collect data from the motional Stark effect (MSE) diagnostic.<sup>23</sup>

### II.B. The Proportional-Integral-Derivative Controller

The formulation of the proportional-integral-derivative (PID) controller is as follows. The error is calculated as

$$e = \beta_{N, request} - LPF(\beta_{N, rEFIT}; \tau_{LPF}) , \quad (1)$$

where  $\beta_{N, request}$  is the requested value of  $\beta_N$  and  $\beta_{N, rEFIT}$  is the value of  $\beta_N$  computed by the rEFIT code.<sup>24</sup> See Ref. 16 for a description of the NSTX rEFIT implementation. The term  $LPF(X; \tau)$  represents a single-pole causal low-pass filter, which is used to eliminate noise in the rEFIT  $\beta_N$  calculation. This filter mimics a simple RC filter and is the solution of

$$\tau_{LPF} \frac{dY_{out}}{dt} + Y_{out} = Y_{in} .$$

This filter form is particularly convenient for implementation in real time, as it can be implemented such that only values from the previous time step need be saved. This can be seen by substituting  $dY_{out}/dt = (Y_{out,i} - Y_{out,i-1})/\delta t$ ,  $Y_{out} = Y_{out,i}$ , and  $Y_{in} = (Y_{in,i} + Y_{in,i-1})/2$  and solving for  $Y_{out,i}$  ( $i$  is a time index):

$$Y_{out,i} = \frac{Y_{out,i-1} + \frac{\delta t}{2\tau_{LPF}} (Y_{in,i} + Y_{in,i-1})}{1 + \frac{\delta t}{\tau_{LPF}}} . \quad (2)$$

This filter helps to smooth out transients in the rEFIT  $\beta_N$ , though at the expense of adding a delay to the system. The value of  $\tau_{LPF}$  is determined by a time-dependent PCS input waveform and is typically set to 10 to 20 ms.

A PID operator is then used to calculate an injected power request, as

$$P_{inj} = P_{\beta_N} \bar{C}_{\beta_N} e + I_{\beta_N} \bar{C}_{\beta_N} \int e dt + D_{\beta_N} \bar{C}_{\beta_N} \frac{de}{dt} + P_{pre-prog} \quad (3)$$

and

$$\bar{C}_{\beta_N} = \frac{I_P V B_T}{200 \mu_0 a \tau_E} . \quad (4)$$

Here, we used  $W = P_{inj}\tau_E$  and  $\beta_T = 2\mu_0 W/VB_T^2$  to relate the injected power and normalized  $\beta$  as  $\beta_N = 200\mu_0 a P_{inj}\tau_E/I_p V B_T = P_{inj}/\bar{C}_{\beta_N}$ , where  $W$  is the total stored energy in the plasma. The parameter  $\bar{C}_{\beta_N}$  is used so that the gain  $P_{\beta_N}$  is dimensionless. Note that these formulas do not take into account any degradation of confinement with input power.<sup>25</sup> The term  $P_{pre-prog}$  denotes a preprogrammed power request. During feedback, this is typically set to a constant equal to the final pre-programmed power value just before feedback is turned on. This helps avoid any instantaneous transients when switching to  $\beta_N$  control, with the integral term ensuring that the error in Eq. (1) goes to zero after sufficient time. The actual values of  $I_p$  and  $B_T$  are used in the real-time calculation of  $\bar{C}_{\beta_N}$ , based on Rogowski coil data from the plasma current and the toroidal field current. Typical values of the volume  $V$  (12 m<sup>3</sup>), minor radius  $a$  (60 cm), and confinement time  $\tau_E$  (40 ms) are fixed in the present version of the code but could also be determined in real time based on information from rtEFIT.

Finally, there is a provision to bypass the PID operator entirely and simply specify an injected power waveform as a function of time. This capability, demonstrated in Sec. IV, provides the ability to program fine power ramps without manually specifying the individual times for the beam modulations.

### II.C. Algorithm Constraints Provided by the NSTX Neutral Beam Hardware

The neutral beam hardware itself<sup>21,22</sup> provides some important technical constraints on the algorithm. The process of forming the neutral beam places significant power on the source grid rails until the beam comes into full focus. The TFTR neutral beams have noncircular molybdenum grid rails as part of the accelerator. These components are not easily remanufactured, so an effort is made to preserve their lifetime by limiting the power flux onto them. Hence, we are presently limiting the system to 20 modulations per source per discharge.

There are also minimum values for the off-time  $\delta t_{off}$  and on-time  $\delta t_{on}$  of the individual sources; the minimum values of these parameters are 10 ms. With regard to the minimum source on duration, it takes a finite time, typically 1 to 2 ms, to form the neutral beam. Beam on-times of <10 ms result in both ambiguity in the actual average injected power and a disproportionate fraction of the total power going into source components and not the plasma. The minimum beam off-time of 10 ms is set by the need to clear the source of the previous plasma before initiating the new arc. Note that the controller to date has used durations of 15 ms or longer for both the minimum on-time and off-time.

Another set of constraints comes from the fact that the arc and filament power supplies for the sources are unregulated, so one source coming on can pull down the voltages for the other sources. Hence, the sources

are tuned for a given order of turn-on, typically source A first, followed by sources B and C. Deliberate or inadvertent deviations from this order can reduce the reliability of the source operations for a given shot. Furthermore, these variations can cause the high-voltage switch tube to oscillate, broadcasting radio-frequency noise into nearby control electronics.

Finally, as presently configured, the  $\beta_N$  controller can only “block” a source, i.e., turn it off. The block can then be removed, allowing the source to turn back on. The initial turn-on of any given source is programmed by the neutral beam operators. There is also an interlock on the system that turns the entire beam system off (with a 50-ms delay) if the plasma current falls beneath 200 kA.

### II.D. The Modulation Scheme

Although the injected power request generated by the PID operator is continuously variable, the neutral beams are not; they can only be on or off. The task of the modulation calculator is to make this translation, while taking into account the constraints of the beam injection hardware. This code is described below.

The controller has a  $3 \times 3$  array specifying the modulation order of the sources; this array can be modified by the physics operator using a standard PCS interface. For example, the typical first row with values [0,1,2] implies that first source A, then B, then finally C will turn on. If the controller requests 5 MW of input power and all sources are at 2 MW, then sources A and B will be fully on, while C will modulate with a 50% duty cycle. The modulations are counted, and if their number exceeds the maximum allowed, then the second row of the modulation order array comes into play. This row is typically filled with [0,2,1], such that the source doing the primary modulations (typically B or C) is switched with the less-used source. The source that has exceeded its allowed number of modulations goes to a default on or off state determined by the physics operator before the discharge is initiated.

Once the duty cycles for the individual sources have been determined from the above steps, the controller decides whether or not to modulate each source. If the duty cycle for a given source is 100% ( $f_{DC} = 1$ ) and the source is already on, it is left on. If that source is off and the time since it was last turned off is  $>\delta t_{off}$ , then it is turned on; otherwise, it is left off. If the duty cycle is 0% ( $f_{DC} = 0$ ) and the source is already off, it is left off. If that source is on and the time since it was last turned on is  $>\delta t_{on}$ , then it is turned off; otherwise, it is left on.

The situation is slightly more complicated for cases with intermediate values of the duty cycle ( $0 < f_{DC} < 1$ ). A quantity  $\Delta$  is computed as

$$\Delta = \max\left(\frac{\delta t_{off}}{1 - f_{DC}}, \frac{\delta t_{on}}{f_{DC}}\right). \quad (5)$$

If the source is on and the time since it was last turned on is  $>f_{DC}\Delta$ , then the source is turned off. If the source is off and the time since it was turned off is  $>(1 - f_{DC})\Delta$ , then the source is turned on.

### III. DETERMINATION OF PID GAINS

A necessary step in the implementation of the controller was to determine the PID gain parameters. We do this by approximating the system with a first-order plus dead time (FOPDT) model,<sup>26</sup> noting that the degradation of confinement with power is an effect that falls outside the model. The system identification and controller tuning are then done with the Ziegler-Nichols (or process-reaction) method,<sup>26</sup> a commonly used open-loop tuning method for FOPDT systems that was previously used for tuning NSTX strike-point position controllers.<sup>27</sup>

In this method, a step is placed in the neutral beam power  $P_{inj}(t)$ , and the details of the  $\beta_N(t)$  response are studied. Three important parameters in the response are then used for tuning the controller. These are the delay between the change in the beam power and the change in  $\beta_N(\tau_{dead})$ , the timescale for the evolution of  $\beta_N(\tau_{\beta_N})$ , and the change of beam power  $(\delta P_{inj})$  normalized to the  $\beta_N$  change  $(\delta P_{inj}/\delta\beta_N)$ . Once these values are determined, the PID parameters can be determined from Table I. Here, we use  $K_0 = (\delta P_{inj}/\delta\beta_N)(\tau_{\beta_N}/\tau_{dead})$ , and the PID operator is defined in Eq. (3).

The step response of the FOPDT system is given by an exponential function, written for the purposes of this study as

$$\beta_N(t) = \begin{cases} \beta_{N,0} & , \quad t < t_{step} \\ \beta_{N,0} + \delta\beta_N \left( 1 - \exp\left(-\frac{t - t_{step} - \tau_{dead}}{\tau_{\beta_N}}\right) \right) & , \quad t > t_{step} \end{cases} \quad (6)$$

Equation (6) is fit to the measured evolution of  $\beta_N$ , where  $\beta_{N,0}$ ,  $\delta\beta_N$ ,  $\tau_{\beta_N}$ , and  $\tau_{dead}$  are fit parameters and  $t_{step}$  is the time of the beam step-up. The fits of Eq. (6) were done

with the Levenberg-Marquardt algorithm<sup>28</sup> as written in the MPFIT curve-fitting libraries.<sup>29</sup> Initial guesses were provided for the parameters  $\beta_{N,0}$ ,  $\delta\beta_N$ ,  $\tau_{\beta_N}$ , and  $\tau_{dead}$ , and the algorithm adjusted them to best match the measured  $\beta_N$  evolution. The times included in the fitting process were from 20 ms before the beam turn-on to 150 ms afterward. We note that although  $\tau_{dead}$  includes the effect of various system delays and  $\tau_{\beta_N}$  is related to the total energy confinement time, these identifications are not strictly correct. Rather, the purpose of the fitting step in Eq. (6) is to identify the characteristics of the first-order system nearest to the actual dynamics in order to design the controller.

Four examples of the application of the method are given in Fig. 2. Each case shows the neutral beam power and the  $\beta_N$  evolution as well as fits to Eq. (6). The plasma currents are indicated in each figure. The fit parameters are shown in the frames and are used with the formulas in Table I to determine the appropriate gain parameters for feedback use.

We have generally chosen to use a proportional-integral controller for experiments in NSTX. Use of a purely proportional controller, with no additional preprogrammed power, causes the achieved steady-state  $\beta_N$  to be less than the request. This can be seen by taking the steady-state-achieved normalized  $\beta$  ( $\beta_{N,achieved}$ ) and relating it to the input power as  $P_{inj} = \bar{C}_A \beta_{N,achieved}$ . The constant  $\bar{C}_A$  is different from  $\bar{C}_{\beta_N}$  above, as the former depends on the actual values of the plasma parameters ( $I_P, B_T, \tau_E$ , etc.), while the latter is a constant in the PCS; the power degradation of confinement is neglected in this simple calculation. Setting this specification for the injected power to be equal to that in Eq. (3) and using proportional gain only allows the ratio of achieved-to-requested  $\beta_N$  to be calculated as  $\beta_{N,A}/\beta_{N,Req} = P_{\beta_N}/(\bar{C}_A/\bar{C}_{\beta_N} + P_{\beta_N})$ . This ratio approaches 1 for arbitrarily large gain, though this might introduce instability into the system. The use of integral gain allows the error to approach zero for reasonable values of proportional gain. Derivative gain was not used, as the  $\beta_N$  signal from rtEFIT is sufficiently noisy that a reliable calculation of  $d\beta_N/dt$  is not possible.

### IV. EXAMPLE USE OF THE ALGORITHM

A detailed example of the algorithm performance for a single discharge is shown in Fig. 3. The discharge in this case is a high-elongation ( $\kappa = 2.5$ ), high-triangularity discharge of the type described in Ref. 30, with  $I_P = 800$  kA. All neutral beams are operated with a voltage of 90 kV, corresponding to 2 MW of injected power per source.

The initial turn-on of the sources is manually programmed, with  $\beta_N$  control starting at  $t = 0.2$  s. The requested  $\beta_N$  is shown in Fig. 3b, as is the low-pass filtered

TABLE I

Determination of the Optimal PID Parameters from the Ziegler-Nichols Method

Controller Type	$P_\beta$	$I_\beta$	$D_\beta$
P	$K_0/\bar{C}_{\beta_N}$	0	0
PI	$0.9K_0/\bar{C}_{\beta_N}$	$0.9K_0/(3.3\tau_{dead}\bar{C}_{\beta_N})$	0
PID	$1.2K_0/\bar{C}_{\beta_N}$	$1.2K_0/(2\tau_{dead}\bar{C}_{\beta_N})$	$1.2\tau_{dead}K_0/(2\bar{C}_{\beta_N})$

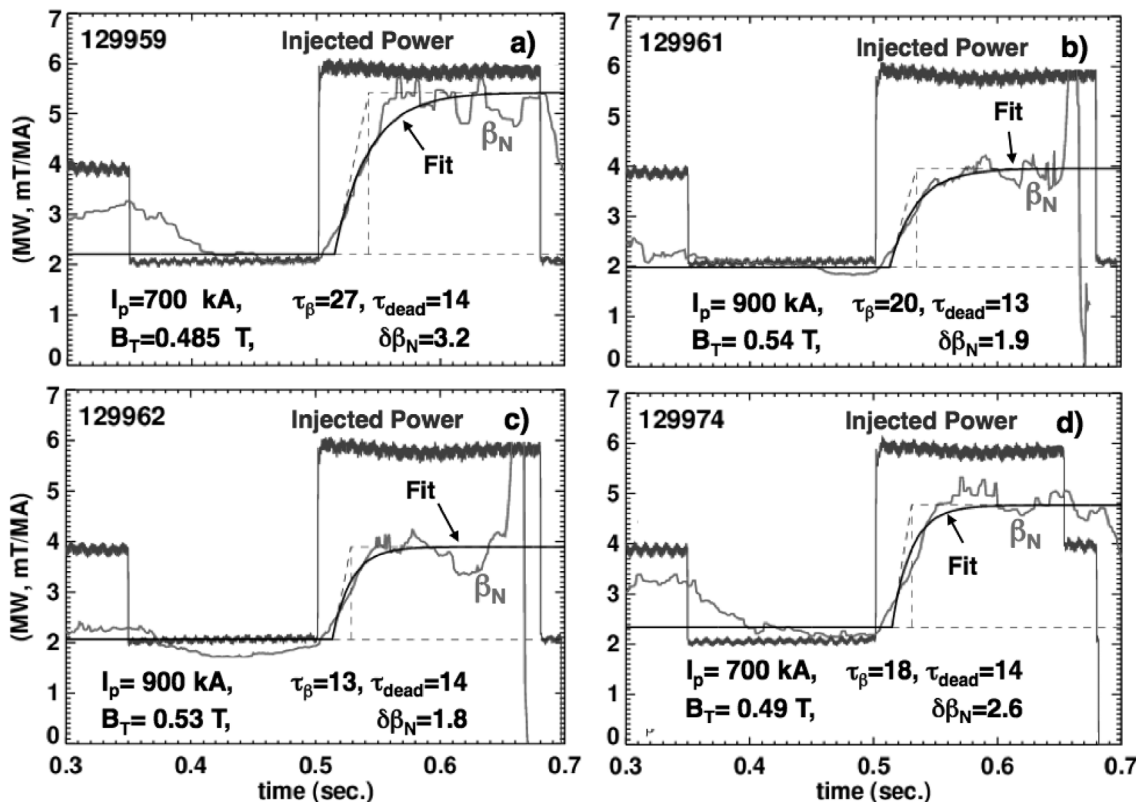


Fig. 2. Example discharges used for open-loop tuning of the  $\beta_N$  controller. Shown are the beam power,  $\beta_N$  evolution, and fits to the  $\beta_N$  evolution. Times displayed in text in the frames are in milliseconds and are rounded to the nearest millisecond. The increment of beam power is 4 MW in all cases.

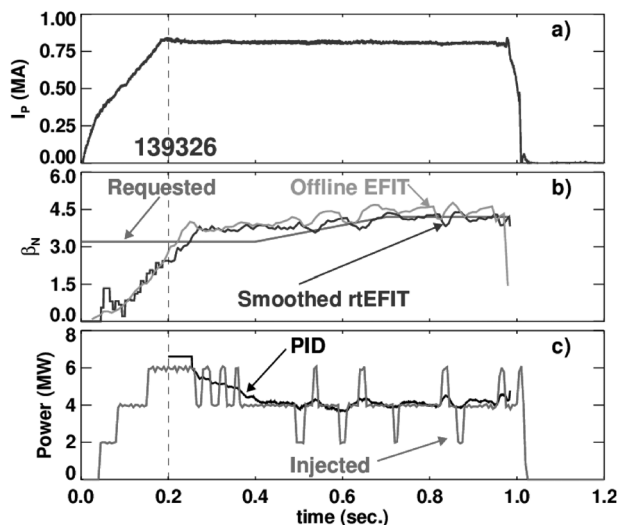


Fig. 3. Demonstration of  $\beta_N$  control in NSTX. Shown are (a) the plasma current; (b) the requested  $\beta_N$ , as well as that calculated by real-time and off-line EFIT; and (c) the requested and actual injected power. Feedback is on from  $t = 0.2$  s onward.

$\beta_N$  from rtEFIT. The requested  $\beta_N$  exceeds the measured value when feedback is first turned on, and the controller leaves all three beam sources on (black trace in Fig. 3c). The achieved  $\beta_N$  quickly exceeds the requested value, and the controller immediately begins to reduce the injected power. The controller reaches near steady state by 500 ms, settling at the  $\sim 4$  MW of input power required to achieve the requested  $\beta_N$ .

Figure 3b also shows the value of  $\beta_N$  calculated by the more accurate off-line EFIT code.<sup>31,32</sup> The off-line calculation is systematically higher than the real-time calculation. The constraint set for the off-line calculation is more comprehensive: The two reconstructions are constrained by similar poloidal field and flux measurements, but the off-line calculation is further constrained by a measurement of the diamagnetic flux and a rough estimate of the pressure profile. Also, unlike the real-time solution, the off-line EFIT is a fully converged solution of the Grad-Shafranov equation. For these reasons, the off-line calculation is a better measure of the true value of  $\beta_N$ . However, when considering a requested  $\beta_N$  evolution, it is necessary to request values consistent with the real-time calculation. We note also that the 15-ms

time constant for the filter in Eq. (1) produces a small time delay in the rtEFIT calculation compared to that using off-line EFIT.

An example application of the algorithm is shown in Fig. 4. This experiment was an attempt to study the onset of  $n = 1$  locked modes as a function of toroidal field and plasma current at constant  $\beta_N$  (Ref. 33); a large  $n = 1$  field was applied after  $t = 0.4$  s, resulting in the eventual development of a locked mode and disruption of the plasma.

The plasma current waveform is shown in Fig. 4a, with a range from 700 to 1100 kA in the study; the toroidal field was also changed from 0.34 to 0.54 T to maintain a constant safety factor. The value of  $\beta_N$  was requested to be 3.2 in all cases. The  $\beta_N$  controller was turned on at  $t = 180$  ms. The beams were preprogrammed to be the same before that time, and as described above, that level of preprogrammed power was left in the  $P_{inj}$  request in Eq. (3) for the remainder of the discharge.

The evolution of  $\beta_N$  is quite different before the controller is turned on, as expected from the change in toroidal field. Once the controller is turned on, beam modulations are used to control the  $\beta_N$  value to the same level. Note that the low-current discharge continues to have a value of  $\beta_N$  somewhat higher than the others. This is because the algorithm is not allowing source A to mod-

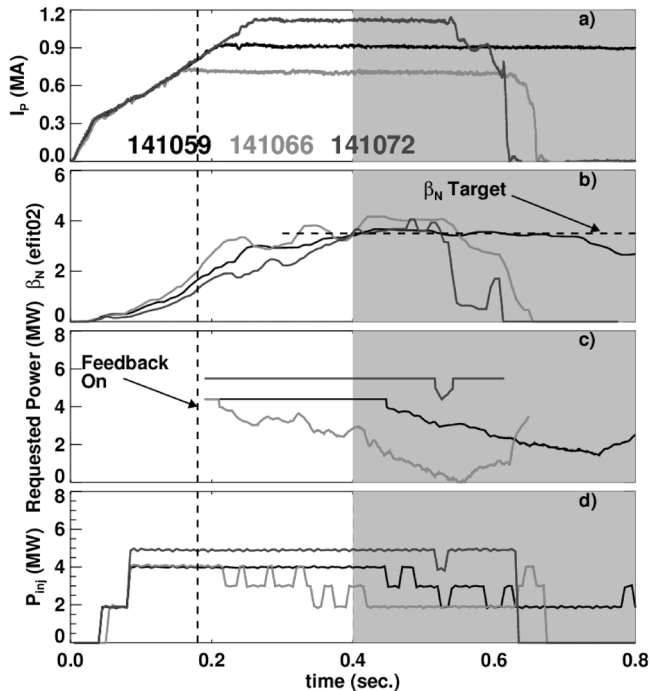


Fig. 4. Demonstration of  $\beta_N$  control in NSTX. Shown are (a) the plasma current, (b)  $\beta_N$ , (c) the requested power, and (d) the actual injected power. Ramping  $n = 1$  fields are applied starting at  $t = 0.4$  s, where the plot becomes gray.

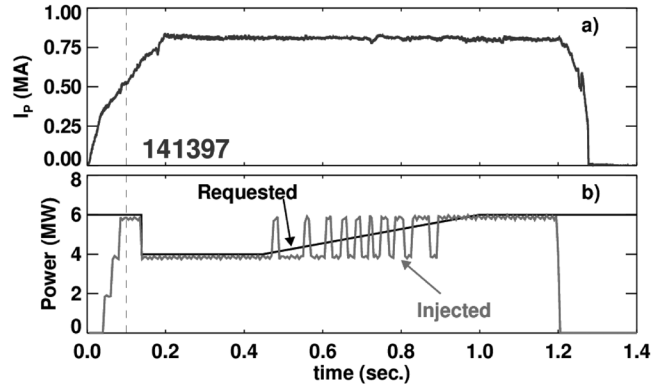


Fig. 5. Demonstration of preprogrammed power ramps. Shown are (a) the plasma current and (b) the requested and injected powers.

ulate, so as not to lose the MSE diagnostic data. We also note that the beam powers for sources B and C were reduced to 1 MW in the 700- and 900-kA cases, to provide a finer power control. The source B power was raised to 2 MW in the 1100-kA case so that sufficient power was available to achieve the requested  $\beta_N$ . Without the controller, multiple discharges would have been needed to determine the necessary beam power waveforms. Use of the controller enabled the experiment to be completed with much greater efficiency. Use of the controller for experiments with  $\beta_N$  nearer to ideal stability limits is described in Refs. 30 and 34.

As noted above, the present software also allows the injected power to be directly specified as an input waveform, with the algorithm then modulating the neutral beams to match the power request. An example of this is shown in Fig. 5. The plasma current is shown in Fig. 5a, while the requested and injected power are shown in Fig. 5b. There is a slow ramp in the request, which the modulation algorithm translates into properly spaced beam modulations. This programming of such modulations would be quite tedious by hand but is made trivial by the present control software.

## V. DISCUSSION

The  $\beta_N$  control system has proven quite useful in NSTX. There are, however, some possible improvements that would further improve performance. These include

1. addition of a causal median filter on the  $\beta_N$  values from rtEFIT. This would help prevent spurious real-time reconstructions, and the associated large error in Eq. (1), from setting off transients in the requested power.
2. a real-time estimation of the confinement time  $\tau_E$  in Eq. (4), based on the input power, stored

energy, and stored energy rate of change. This would allow the proportional and integral gain parameters to be more effectively constant over a range of plasma parameters.

- improvement of the real-time calculation of  $\beta_N$ , either through improvements to the actual Grad-Shafranov calculation (more appropriate basis functions for  $ff'$  and  $p'$ , for instance) or by adding additional data constraints. Improvement here would likely also help with other controllers that use the rtEFIT output, such as the ISOFLUX shape controller.<sup>16</sup>

A more fundamental limit on the algorithm comes from the observation that the disruptive  $\beta_N$  limit is not constant. For instance, the achievable stable  $\beta_N$  is known to be a strong function of parameters such as the pressure peaking factor and internal inductance<sup>2,35-39</sup> and plasma shape.<sup>2,38,40,41</sup> Furthermore, in the presence of an imperfectly conducting wall, the plasma will be unstable to a resistive wall mode,<sup>42,43</sup> a pressure or current-driven kink instability growing on the  $L/R$  time of the conducting wall. Hence, the operator of the algorithm must know exactly what  $\beta_N$  to request for a given plasma configuration. This problem could be eliminated by doing feedback on some variable even more sensitive to the plasma proximity to instability than  $\beta_N$ . Such a method was proposed in Ref. 44, where the plasma amplification of an applied  $n = 1$  field was suggested as a sensitive measure of the stability of the plasma. The present  $\beta_N$  control system is a first step toward implementing an advanced magnetohydrodynamic controller of this sort. It also provides the groundwork for current profile control in NSTX-Upgrade.<sup>45</sup>

## ACKNOWLEDGMENTS

The authors thank L. Grisham and S. Kaye for helpful discussion and the neutral beam and plasma operations groups for their technical support in the implementation of this system. This research was funded by the U.S. Department of Energy under contract DE-AC02-09CH11466.

## REFERENCES

- M. SUGIHARA, *Nucl. Fusion*, **47**, 337 (2007).
- E. J. STRAIT, *Phys. Plasmas*, **1**, 1415 (1994).
- M. ONO et al., *Nucl. Fusion*, **40**, 557 (2000).
- G. L. CAMPBELL et al., "New DIII-D Tokamak Plasma Control System," *Proc. 17th Symp. Fusion Technology*, Rome, Italy, September 14-18, 1992, Vol. 2, p. 1017 (1992).
- J. E. LAWSON et al., "Beta Normal Control of TFTR Using Fuzzy Logic," *Proc. 18th Symp. Fusion Technology*, Karlsruhe, Germany, August 22-26, 1994, Vol. 1, p. 739 (1994).
- N. H. ZORNIG et al., "Experimental Results Using the JET Real Time Power Control System," *Proc. 19th Symp. Fusion Technology*, Lisbon, Portugal, September 16-20, 1996, Vol. 1, p. 705 (1996).
- T. OIKAWA et al., *Fusion Eng. Des.*, **70**, 175 (2004).
- Y. NEYATANI et al., *Fusion Eng. Des.*, **36**, 429 (1997).
- T. SCOVILLE et al., *Fusion Eng. Des.*, **82**, 1045 (2007).
- J. R. FERRON et al., *Nucl. Fusion*, **46**, L13 (2006).
- D. MOREAU et al., *Nucl. Fusion*, **43**, 870 (2003).
- D. GATES et al., *Fusion Eng. Des.*, **81**, 1911 (2006).
- D. MASTROVITO et al., *Fusion Eng. Des.*, **85**, 447 (2010).
- B. G. PENAFLORE et al., "A Structured Architecture for Advanced Plasma Control Experiments," *Proc. 19th Symp. Fusion Technology*, Lisbon, Portugal, September 16-20, 1996, p. 965 (1996).
- B. G. PENAFLORE et al., *Fusion Eng. Des.*, **71**, 47 (2004).
- D. A. GATES et al., *Nucl. Fusion*, **46**, 17 (2006).
- J. E. MENARD et al., *Nucl. Fusion*, **50**, 045008 (2010).
- S. P. GERHARDT et al., *Plasma Phys. Control. Fusion*, **52**, 104003 (2010).
- S. A. SABBAGH et al., *Phys. Rev. Lett.*, **97**, 045004 (2006).
- S. A. SABBAGH et al., *Nucl. Fusion*, **50**, 025020 (2010).
- T. STEVENSON et al., "A Neutral Beam Injector Upgrade for NSTX," PPPL-3651, Princeton Plasma Physics Laboratory (Jan. 2002).
- L. R. GRISHAM and TFTR GROUP, *Plasma Devices Operations*, **3**, 187 (1994).
- F. LEVINTON and H. YUH, *Rev. Sci. Instrum.*, **79**, 10F522 (2008).
- J. R. FERRON et al., *Nucl. Fusion*, **38**, 1055 (1998).
- E. J. DOYLE et al., *Nucl. Fusion*, **47**, S18 (2007).
- D. XUE, Y. Q. CHEN, and D. P. ATHERTON, *Linear Feedback Control: Analysis and Design with MATLAB (Advances in Design and Control)*, Society for Industrial and Applied Mathematics, Philadelphia, Pennsylvania (2008).
- E. KOLEMEN et al., *Nucl. Fusion*, **50**, 105010 (2010).
- P. R. BEVINGTON and D. K. ROBINSON, *Data Reduction and Error Analysis for the Physical Sciences*, McGraw-Hill, Boston, Massachusetts (1992).

Gerhardt et al.  $\beta_N$  CONTROL IN NSTX

29. C. B. MARKWARDT, "Non-Linear Least Squares Fitting in IDL with MPFIT," *ASP Conf. Ser.*, Vol. 411, p. 251, D. BOHLENDER, P. DOWLER, and D. DURAND, Eds., see also <http://purl.com/net/mpfit> (current as of Oct. 5, 2010).
30. S. P. GERHARDT et al., "Progress in the Development of Advanced Spherical Torus Operating Scenarios in NSTX," presented at 23rd International Atomic Energy Agency Fusion Energy Conf., Daejeon, South Korea, October 11–16, 2010.
31. S. A. SABBAGH et al., *Nucl. Fusion*, **41**, 1601 (2001).
32. S. A. SABBAGH et al., *Nucl. Fusion*, **46**, 635 (2006).
33. R. J. BUTTERY et al., "The Impact of 3D Fields on Tearing Mode Stability of H-Modes," presented at 23rd International Atomic Energy Agency Fusion Energy Conf., Daejeon, South Korea, October 11–16, 2010.
34. S. A. SABBAGH et al., "Resistive Wall Mode Stabilization and Plasma Rotation Damping Considerations for Maintaining High Beta Plasma Discharges in NSTX," presented at 23rd International Atomic Energy Agency Fusion Energy Conf., Daejeon, South Korea, October 11–16, 2010.
35. W. HOWL et al., *Phys. Fluids B*, **4**, 1724 (1992).
36. J. E. MENARD et al., *Nucl. Fusion*, **37**, 595 (1997).
37. J. E. MENARD et al., *Nucl. Fusion*, **43**, 330 (2003).
38. J. E. MENARD et al., *Phys. Plasmas*, **11**, 639 (2004).
39. S. A. SABBAGH et al., *Nucl. Fusion*, **44**, 560 (2004).
40. E. LAZARUS et al., *Phys. Plasmas B*, **3**, 2220 (1991).
41. D. A. GATES et al., *Phys. Plasmas*, **13**, 056122 (2006).
42. A. BONDESON and D. J. WARD, *Phys. Rev. Lett.*, **72**, 2709 (1994).
43. A. C. SONTAG et al., *Nucl. Fusion*, **47**, 1005 (2007).
44. H. REIMERDES et al., *Nucl. Fusion*, **45**, 368 (2005).
45. J. E. MENARD et al., "Physics Design of NSTX Upgrade," *Proc. 37th European Physical Society Conf. Plasma Physics*, Dublin, Ireland, June 21–25, 2010; <http://ocs.ciemat.es/EPS2010PAP/pdf/P2.106.pdf> (current as of Oct. 5, 2010).